THE JOURNAL OF PHYSICAL CHEMISTRY A

Article

pubs.acs.org/JPCA

Order of Magnitude Dissociative Ionization Enhancement Observed for Pulses with High Order Dispersion

Muath Nairat,[†] Vadim V. Lozovoy,[†] and Marcos Dantus*[,†,‡]

[†]Department of Chemistry, Michigan State University, East Lansing, Michigan 48824, United States

[‡]Department of Physics and Astronomy, Michigan State University, East Lansing, Michigan 48824, United States

Supporting Information

ABSTRACT: While the interaction of atoms in strong fields is well understood, the same cannot be said about molecules. We consider how dissociative ionization of molecules depends on the quality of the femtosecond laser pulses, in particular, the presence of third- and fourth-order dispersion. We find that high-order dispersion (HOD) unexpectedly results in order-of-magnitude enhanced ion yields, along with the factor of 3 greater kinetic energy release compared to transform-limited pulses with equal peak intensities. The magnitude of these effects is not caused by increased pulse duration. We evaluate the role of pulse pedestals produced by HOD and other pulse shaping approaches, for a number of molecules including acetylene, methanol, methylene chloride, acetonitrile, toluene, and *o*-nitrotoluene, and discuss our findings in terms of processes such as prealignment, preionization, and bond softening. We conclude, based on the quasi-symmetric temporal dependence of the observed enhancements that cascade ionization is likely responsible for the large accumulation of charge prior to the ejection of energetic fragments along the laser polarization axis.

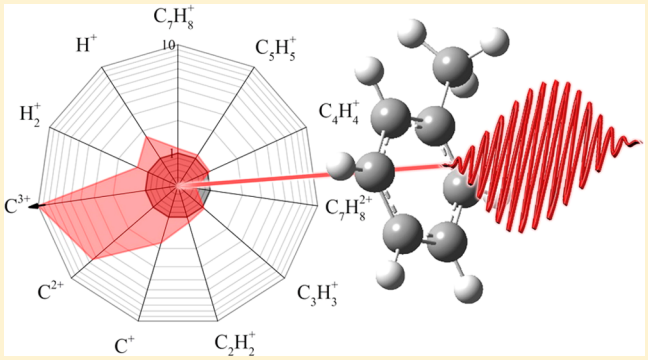

INTRODUCTION

Ultrashort intense femtosecond pulses with peak intensities higher than 10^{13} W/cm^2 have associated field-strength of ∼1 V/Å. Their interaction with matter, while simpler to understand for atoms, is much more complex for molecules.[1−8] Molecules produce multiply charged species and change their molecular structure through the following: deformation, isomerization, and the migration of atoms between different sites within the charged molecule.[9−15] Understanding and controlling these chemical processes with ultrafast laser pulses has been an ongoing dream in the field since the 1980s.[5,6,16−19]

Strong field ionization is largely determined by the peak intensity and the duration of the laser field. Within a few cycles, the electric field is able to overcome molecular bonds and cause dissociation. Efficient proton elimination with high excess energy from molecules is often observed.[11,20] A number of models have been considered to explain dissociative ionization of molecules under intense fields. One such model posits that the process is ruled by stretching of C−H bonds.[21] As the duration of pulse increases, bond-lengths reach a critical internuclear distance from which ionization cross section is greater. Another model proposes hydrocarbons ionize to a high-charge state and dissociate in a concerted Coulombic explosion.[11] At the leading edge of the pulse, C−H bonds stretch and the molecule is ionized multiple times. After this event, the skeleton of the molecule Coulomb explodes and forms highly charged fragments. Both of these models depend on pulse duration to explain the dissociative ionization processes.

With the advent of pulse shapers capable of preparing well-defined laser pulses, in terms of phase, amplitude, and polarization;[22] understanding dissociative ionization in greater detail has become possible. Here we explore if the presence of low-intensity pedestals in the pulse, caused by high-order dispersion (HOD), influences the strong-field dissociative ionization of molecules. We focus on HOD because of its natural prevalence in ultrafast laser systems.

The electric field distribution in time domain for a broadband laser pulse with an angular frequency ω can be expressed as

$$E(t) = \int_{-\infty}^{\infty} E(\omega) e^{-i\omega t}\, d\omega \tag{1}$$

where

$$E(\omega) = e^{-1/2(\omega-\omega_0)^2\tau_0^2} e^{i\varphi(\omega)} \tag{2}$$

in which $\tau_0 = \frac{\tau_{fwhm}}{2\sqrt{\ln(2)}}$, τ_{fwhm} is the pulse duration at fwhm. The term $\varphi(\omega)$ is known as the phase of the pulse and can be expanded as

Received: August 28, 2016
Revised: October 13, 2016
Published: October 16, 2016

DOI: 10.1021/acs.jpca.6b08659
J. Phys. Chem. A 2016, 120, 8529−8536

$$\varphi(\omega) = \varphi^{(0)} + \frac{\varphi^{(1)}(\omega - \omega_0)}{1} + \frac{\varphi^{(2)}(\omega - \omega_0)^2}{2!} + \frac{\varphi^{(3)}(\omega - \omega_0)^3}{3!} + \frac{\varphi^{(4)}(\omega - \omega_0)^4}{4!} + \dots \quad (3)$$

The first term $\varphi^{(1)}$ corresponds to a time delay for all the frequencies; the second term $\varphi^{(2)}$ corresponds to the second order dispersion (SOD), also known as chirp. Chirp causes a temporal broadening of the pulse and a change in the arrival order of frequencies in accordance with the phase sign. Using chirp to control the fragmentation of a dissociative event has been studied extensively during the past 20 years.[23−25] Work from this group showed that there is a trend that applies to substantially all molecules; 16 different molecules were studied, and the extent of fragmentation was dictated by the pulse duration.[5] Terms higher than $\varphi^{(2)}$ are referred to as high-order dispersion. For instance, third order dispersion (TOD) causes the appearance of a pedestal before (when negative) or after (when positive) the main pulse, and fourth order dispersion (FOD) causes the appearance of a symmetrical pedestal on both sides of the main pulse. While a great deal of research has been conducted using chirped pulses, few reports explore the role of high-order dispersion in dissociative ionization. The effect of negative TOD on the dissociation of H_2^+ was an increase in ion yields due to prealignment caused by the prepulse pedestal.[26] Whereas negative TOD was found to suppress the nonsequential ionization of the anion SF_6^-.[27]

Here we explore whether the pulse pedestal resulting from HOD influences the dissociative ionization of large molecules. Our interest stems from the fact that HOD is technically challenging to measure and eliminate. Therefore, if an effect is found, it is likely relevant to previous and future experiments with intense femtosecond laser pulses. Moreover, it can help understand the interaction between molecules and intense laser fields.

EXPERIMENTAL METHODS

The experimental setup used here consists of a regeneratively amplified Ti:sapphire laser (Spitfire, Spectra Physics, Santa Clara, CA) producing femtosecond pulses at 1 kHz repetition rate. The near-Gaussian pulses were centered at 800 nm and had a 25.8 nm bandwidth fwhm. The pulses were compressed and shaped after the amplifier using a pulse shaper (MIIPS-HD, Biophotonic Solutions Inc., East Lansing, MI) utilizing the Multiphoton Intrapulse Interference Phase Scan (MIIPS) method.[28,29] The pulse bandwidth corresponds to 36 fs (fwhm) when compressed to transform-limited (TL). The shaper was also used to introduce TOD and FOD phase masks. Amplitude correction was implemented by increasing the transmission value for the HOD pulses relative to the TL pulses without changing the laser spectrum (Figure S1, Supporting Information). This was used to ensure the peak intensity for the phase shaped pulses was the same as that for the TL pulses. The amplitude mask value is based on the theoretical change in the pulse peak intensity while introducing the HOD phase. This was verified experimentally based on the total SHG signal that is obtained from TL, HOD phase only, and amplitude corrected HOD pulses which are also compared to the theoretical SHG signal based on the laser spectrum. High fidelity (pulse-to-pulse stability) of the laser and the absence of pre/post pulses were ensured and confirmed via the fidelity assessment procedure[30,31] (Figure S2).

The experiments were carried out using a Wiley−McLaren time-of-flight mass spectrometer (TOF−MS) having a 0.5 m long field free drift region. The MS chamber was maintained under high vacuum with a base pressure of 6−8 × 10^{-9} Torr. The samples were outgassed by repeated freeze−thaw cycles under vacuum. After outgassing, the samples were introduced into the vacuum chamber via a leak valve and the pressure was maintained at 5 × 10^{-6} Torr, under fast flow condition. Laser pulses were focused onto the effusive sample using a 300 mm achromatic lens. The experiments were carried out at pulse energies corresponding to peak intensities of 1.7, 3.4, 5.1, and 6.8 × 10^{14} W/cm^2. The pulses were linearly polarized in parallel to the TOF−MS and the ion detection axis. The ion extraction plates were 1 cm apart and the DC extraction field between the repeller and the extractor was set at 320 V/cm, while the extractor was kept at 1880 V. The extractor plate consisted of a 0.9 mm wide slit that is perpendicular to the laser propagation axis to ensure ion extraction from the central part of the focused beam and mitigate volume ionization effects.[32−34] The zero-voltage ground plate was a 16 mm diameter circular wire grid placed 1 cm away from the extractor plate. Ions were detected using a 500 MHz digital oscilloscope coupled with dual microchannel plates (MCP's) in Chevron configuration. The MCP's were located at the end of the field-free drift region of the TOF−MS. For each peak intensity value, the resulting ions from 1000 laser shots were collected and averaged. The data acquisition program collected the averaged signal for each of the different phases being evaluated in close succession, in order to prevent the influence of long-term drifts in the signal. This procedure, evaluating multiple different phases, was repeated to obtain 500 averages for each phase.

The effect of high-order dispersion on a femtosecond pulse is relatively subtle and not easy to characterize. We recorded interferometric autocorrelations (AC) for the four types of pulses considered in this research; they are TL, −3 × 10^4 fs^3 TOD, 3 × 10^4 fs^3 TOD, and 3 × 10^6 fs^4 FOD as shown in Figure 1. For the case of TOD pulses, a cross-correlation with a TL pulse is presented. The cross correlation measurement (TL

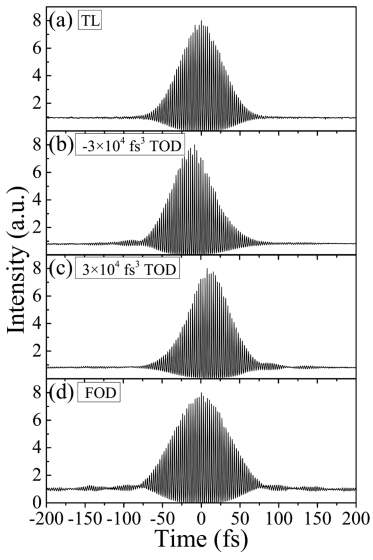

Figure 1. Interferometric AC for (a) TL, (b) −3 × 10^4 fs^3 TOD, (c) 3 × 10^4 fs^3 TOD, and (d) 3 × 10^6 fs^4 FOD pulses. The TOD traces are cross-correlations with TL pulses to show the asymmetric time profiles.

DOI: 10.1021/acs.jpca.6b08659
J. Phys. Chem. A 2016, 120, 8529−8536

vs TOD pulses) are carried out by the pulse shaper and a method called multiple independent comb shaping (MICS).[35] The cross-correlation reveals the asymmetric temporal profile for the pulses and confirms the pedestals for positive and negative TOD has mirror image symmetry (Figure S3). HOD introduces a small pedestal, and some pulse broadening. The retrieved pulse durations (fwhm) are 36, 48, and 64 fs for each phase, respectively. For all our experiments, the peak intensity of the pulses, with or without HOD, was kept constant.

The pedestals seem to be negligible in the autocorrelations shown in Figure 1. For this reason, we plot calculated pulse profiles in logarithmic scale in Figure 2. FOD causes a time-

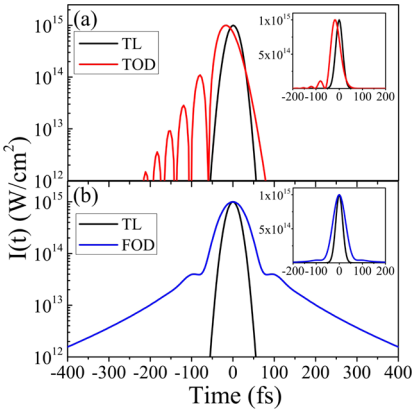

Figure 2. Theoretical simulation for the intensity of TL pulses compared to that of (a) -3×10^4 fs^3 TOD and (b) 3×10^6 fs^4 FOD pulses. The insets show same pulses on a linear scale. Positive TOD (not shown) resembles the negative TOD shown in part a except that the pedestal appears after the main pulse.

symmetric pedestal, while TOD causes a leading (negative) or following (positive) pedestal. The intensity of these pedestals is about 1−2 orders of magnitude smaller than the main pulse and extends for about 200 fs. In strong field laser experiments, where the peak intensity can exceed 1×10^{15} W/cm^2 (as shown in Figure 2), these pedestals cannot be ignored. Our experiments track the dissociative ionization process observed for a number of molecules including acetylene, methanol, methylene chloride, acetonitrile, toluene, and *o*-nitrotoluene; comparing results for TL pulses and pulses with HOD. Our presentation begins by describing in detail results for toluene and *o*-nitrotoluene; we then generalize to the other molecules.

RESULTS

The mass spectrum from toluene using TL pulses at 6.8×10^{14} W/cm^2 is shown in Figure 3 (*o*-nitrotoluene mass spectrum is shown in Figure S4). Both are in good agreement with previous studies.[5,36,37] The strong nonresonant fragmentation of both molecules produces shorter hydrocarbons along with multiply charged ions. Coulomb explosion products can be identified in the spectrum because of their structure; ions traveling toward the detector arrive at earlier times compared to backward moving ions. When comparing the two compounds, *o*-nitrotoluene, which is more polarizable than toluene and has an ionization potential that is larger by 0.4 eV,[38] produces larger amounts of fragment ions relative to that of the molecular ion.[5]

Our results are depicted in logarithmic spider plots in Figure 4 for toluene and Figure 5 for *o*-nitrotoluene. On the basis of this plotting scheme,[39] where ion yields are normalized to

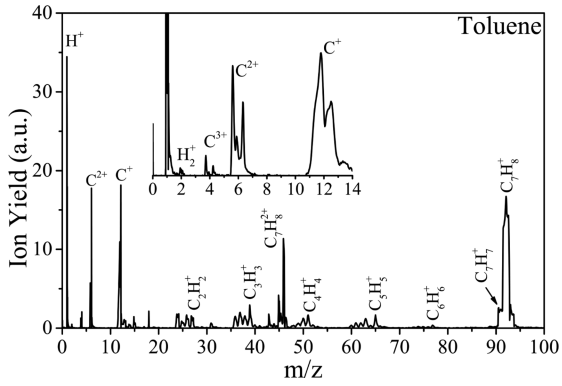

Figure 3. TOF mass spectrum for toluene. The inset in the spectrum shows magnified region over the small m/z fragments.

yields obtained from TL pulses at the given intensity, the mass spectrum using TL pulses is represented as a unity circle. This allows one to determine the relative associated changes in the ion yields when using HOD pulses. Each of the spider plots represents the variations in the relative yield at a particular peak intensity.

At the lowest peak intensity (Figure 4a), one can clearly see yield enhancements resulting from HOD for all of the observed fragment ions, which are the H^+ ion and the heavy fragments. Note that at the lowest intensities some ions are not observed and those are marked by red dots. Comparing between negative (prepedestal) and positive (post- pedestal) TOD, slightly higher enhancement is observed for pulses with a prepedestal. In the case of FOD, symmetrical pedestal, the ion yields were much higher than TL or TOD pulses. With respect to TL, FOD enhancement of several ions, exceeds an order of magnitude; which is represented by the small black arrows in Figure 4a. At higher peak intensities Figure 4b−d, the same trend is observed. The highest overall enhancement occurs when using FOD pulses, whereas negative TOD produces slightly more ions compared to positive TOD. The general enhancement pattern at different peak intensities can be summarized as follows: (i) At any peak intensity, the ions yield increases in the following order: TL < positive TOD < negative TOD < FOD. (ii) At low peak intensity, the heavy fragments and H^+ experience the greatest increase in yield. (iii) At higher peak intensities, the lower m/z fragments (C^+, C^{2+}, C^{3+}) are enhanced.

Similar behavior was observed for *o*-nitrotoluene as shown in the Spider plots in Figure 5. The general trend in the ion yields enhancement is similar to toluene. The highest observed ion yields were observed when using FOD pulses as well. Slight enhancement is observed for negative relative to positive TOD. The observed HOD enhancements are slightly lower than those noted in the case of toluene.

Similar experiments were carried out on a number of different molecules. The dissociative ionization of acetylene, methanol, methylene chloride, and acetonitrile showed, in general, similar ion yields enhancement as described for the larger mollecules. Here we only show in detail results for acetylene in Figure 6. As for the other molecules, at low intensity factor-of-10 enhancement is observed for the parent ion. At higher intensities, the over an order-of-magnitude enhancement is observed for C^{2+} and, in the case of acetylene, for the doubly charged acetylene ion. Formation of acetylene dication, at mass-to-charge 13, is distinguished from the CH^+

DOI: 10.1021/acs.jpca.6b08659
J. Phys. Chem. A 2016, 120, 8529−8536

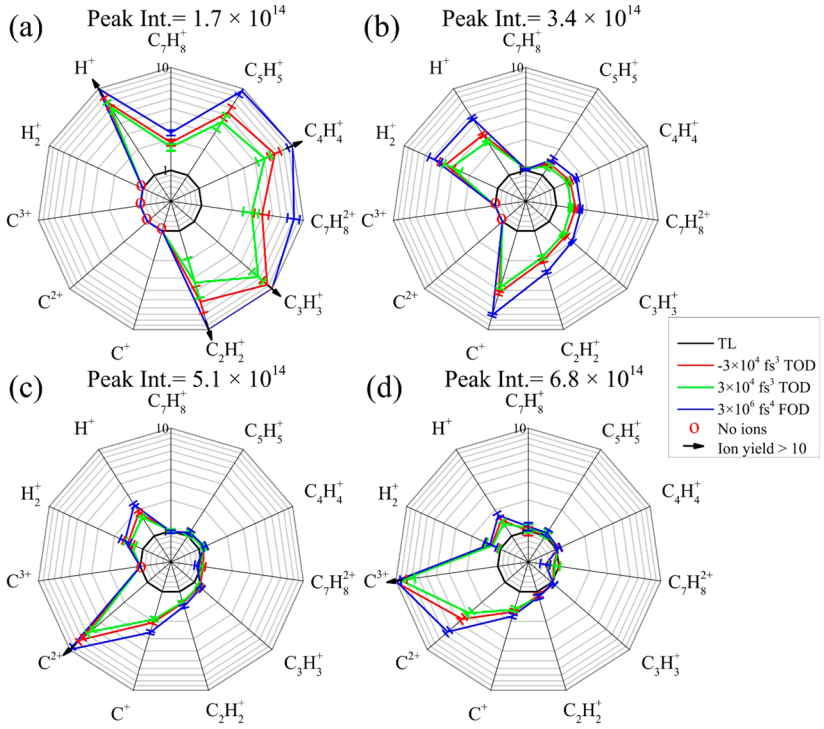

Figure 4. Spider plots on a logarithmic scale for the observed toluene fragment ions using FOD (blue), negative (red), and positive (green) TOD pulses compared to TL (black) pulses at (a) 1.7, (b) 3.4, (c) 5.1, and (d) 6.8×10^{14} W/cm^2 peak intensity. The ion yield enhancements indicated by the black arrows using FOD are (a) $C_4H_4^+ = 12.5 \pm 1.0$, $C_3H_3^+ = 18.4 \pm 1.6$, $C_2H_2^+ = 14.6 \pm 1.9$, and $H^+ = 20 \pm 2$, (c) $C^{2+} = 13.7 \pm 0.8$, and (d) $C^{3+} = 16 \pm 1$.

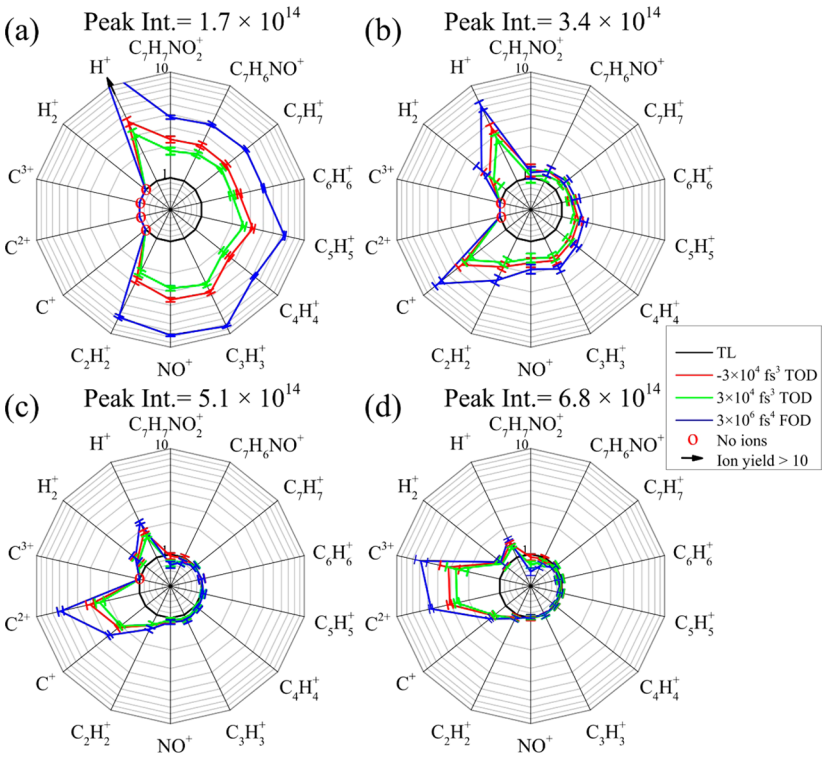

Figure 5. Spider plots on a logarithmic scale for the observed *o*-nitrotoluene fragment ions using FOD (blue), negative (red) and positive (green), TOD pulses compared to TL (black) pulses at (a) 1.7, (b) 3.4, (c) 5.1, and (d) 6.8×10^{14} W/cm^2 peak intensity. The ion yield enhancements indicated by the black arrows using FOD in part a are $H^+ = 15.9 \pm 1.0$.

fragment ion, based on the appearance of a small peak at mass-to-charge 13.5 corresponding to ^{13}C containing doubly charged acetylene ions with an intensity pattern that matches the relative natural abundance of the carbon isotope. Double ionization of acetylene requires ~32 eV, and its ground state is stable.[40] Dissociative enhancement associated with HOD

DOI: 10.1021/acs.jpca.6b08659
J. Phys. Chem. A 2016, 120, 8529−8536

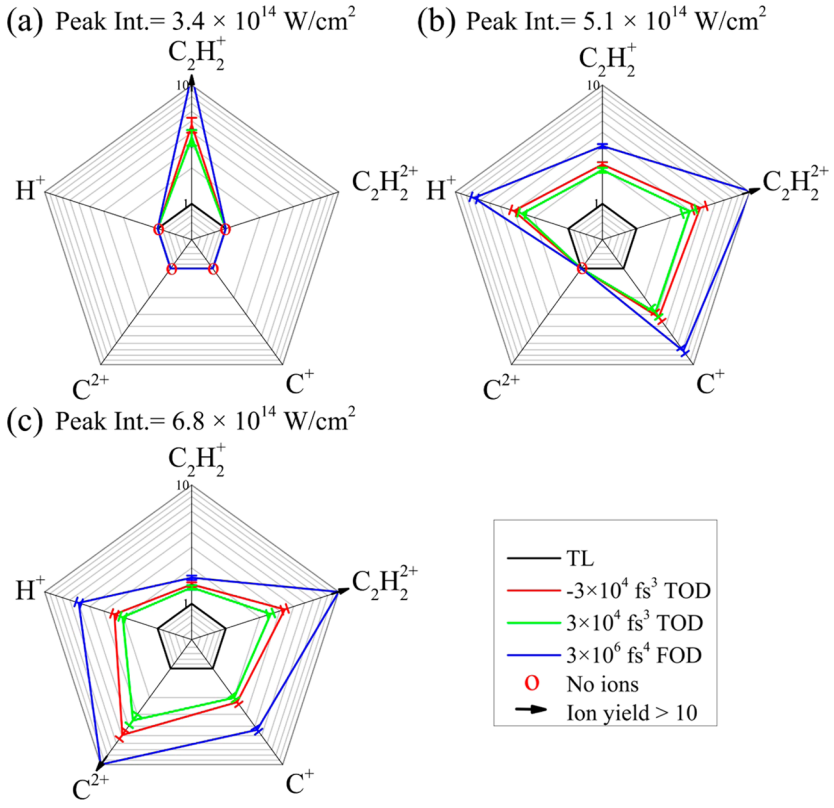

Figure 6. Spider plots on a logarithmic scale for the observed acetylene fragment ions using FOD (blue), negative (red), and positive (green) TOD pulses compared to TL (black) pulses at (a) 3.4, (b) 5.1, and (c) 6.8 × 10^{14} W/cm^2 peak intensity. The ion yield enhancements indicated by the black arrows using FOD are (a) $C_2H_2^+$ = 12.2 ± 0.8, (b) $C_2H_2^{2+}$ = 10.2 ± 0.9, and (c) $C_2H_2^{2+}$ = 12.2 ± 0.7 and C^{2+} = 16.5 ± 1.2.

occurs with the smaller molecules at slightly higher intensities compared to the larger ones. Moreover, the proton ion yield enhancement (compared to TL at any given peak intensity) was also smaller and was found to increase in the following order: methylene chloride < acetonitrile < acetylene < methanol.

Kinetic energy release (KER) following dissociative ionization was obtained from the measured peak profiles for the light fragments, which appear as multiple separate components due to the fact that the forward Coulomb exploded fragments reach the detector at an earlier time compared to the backward ones (see Figure 3). From such peak profiles, the KER can be calculated according to the equation:[41]

$$\mathrm{KER\ (eV)} = 9.65 \times 10^{-7} \frac{\Delta t^2 n^2 F^2}{8m} \tag{4}$$

where Δt is the separation time between the forward and backward peaks in nanoseconds, n is the charge, F is the DC extraction field in V/cm, and m is the atomic mass number. The KER distributions are obtained from the forward ion peaks in Figure 7, in order to circumvent the limited angular acceptance in the ion spectrometer over the energetic fragments. The calculated KER distributions was obtained at 6.8 × 10^{14} W/cm^2 for the forward peaks of H^+, C^{3+}, and C^{2+} from toluene and *o*-nitrotoluene while using vertically polarized beam (parallel to the flight tube and the detection axis). When horizontally polarized beam was used, the total ion yields and their KER were limited to the less energetic fragments (Figures S5 and S6). HOD increases the total ion yields as well as the KER distribution. This is observed regarding both the cutoff KER

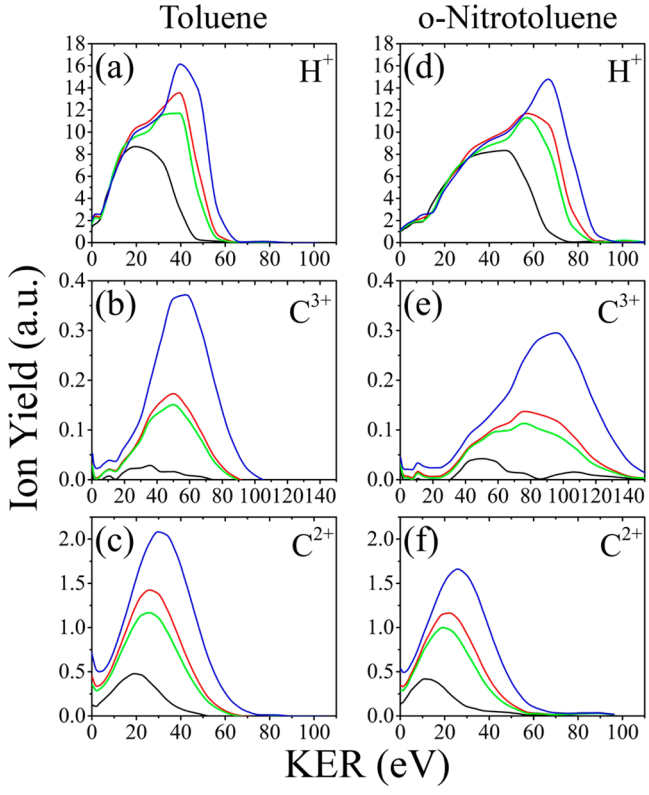

Figure 7. KER from (a–c) toluene and (d–f) *o*-nitrotoluene using TL (black), positive (green) and negative (red) TOD, and FOD (blue) pulses at 6.8 × 10^{14} W/cm^2 peak intensity.

DOI: 10.1021/acs.jpca.6b08659
J. Phys. Chem. A 2016, 120, 8529–8536

and the most probable KER. A similar behavior is observed for C^{3+} and C^{2+}.

A similar increase in the KER of H^+, C^{2+}, and C^+ was found for acetylene (Figure 8), and for the other smaller molecules.

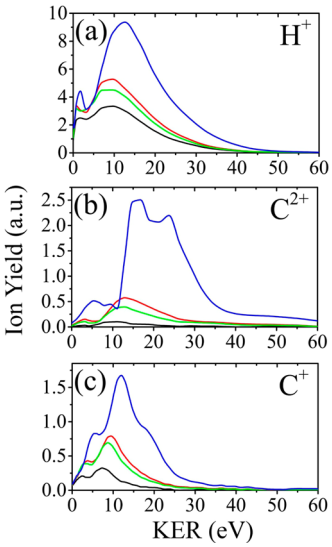

Figure 8. KER from acetylene using TL (black), positive (green) and negative (red) TOD, and FOD (blue) pulses at 6.8×10^{14} W/cm^2 peak intensity.

The increase in KER associated with the presence of HOD indicates greater accumulation of charge prior to Coulomb explosion. The increase in both of the total amount of fragments and their KER indicates a significant role for the pedestal in the dissociation mechanism The KER cutoff values from acetylene and the other small molecules were smaller than those observed for the larger molecules. The KER increase appears to depend on the number of charges that can be accumulated prior to Coulomb explosion, as discussed below.

DISCUSSION

To understand the underlying mechanism behind the observed yield and KER enhancements reported for pulses with HOD, we draw from previous findings in the strong field ionization literature. Ionization processes are highly dependent on the relative orientation of the molecule and the laser polarization axis.[42] Pulses with negative TOD have been implemented to increase the dissociation yield of H_2^+[26] by means of using the pedestal to induce nonadiabatic alignment of the molecule. Such a mechanism is feasible in the case of small diatomic molecules, where the rotational constant supports fast rotation within the time scale of the pedestal. In the current work with large molecules, the rotational constants are associated with a rotational motion that is 2 orders of magnitude slower. Therefore, it is unlikely that significant alignment is induced by the prepedestal. Moreover, one would expect to have a greater difference between negative and positive TOD, whereas only slight enhancement was observed in the favor of negative TOD.

It has been shown that when the molecular bonds get stretched to a certain critical internuclear distance "bond softening", ionization cross section reaches a peak rate that is orders of magnitude larger than at the equilibrium internuclear distance.[43] This process is also known as enhanced ionization and is attributed mainly to the nonadiabatic electron density localization near the nuclei after bond stretching. The enhanced ionization mechanism has been used to explain the ejection of energetic H^+ from polyatomic hydrocarbons due to the accumulation of a highly charged parent ion.[11] With increasing molecular size, bond softening can occur at multiple C−H bonds simultaneously, leading to a highly charged state with strong Coulomb repulsion forces. The highly charged state mechanism, in which all the H^+ fragments are ejected at once in a concerted fashion, has been demonstrated in the framework of time-dependent Hartree−Fock[44] and time-dependent density functional theories.[45,46] In our current work, the ejection of energetic H^+ can be explained to take place following a similar mechanism, which is supported by the increased KER values with accordance to the molecular size.

TOD and FOD pulses are associated with the presence of pedestals along with a slight increase in the pulse duration. An increase in the yield of energetic H^+ ejection from molecules has been observed to occur at constant intensity with longer pulse durations.[21] The observation was attributed to the necessity to populate the precursor's highly charged states through which multiple C−H stretching and softening can occur, followed by the concerted Coulomb explosion. However, the currently observed enhancement, both in terms of yield and kinetic energy, is attributed mainly to the pulse pedestals. We confirm this assertion by plotting changes in the ion yields when employing TL pulses with durations that are similar to that of the TOD and FOD. Such changes were much smaller than those found for TOD and FOD pulses (see Figure S7).

The higher KER values are consistent with HOD pedestals leading to highly charged precursors prior to Coulomb explosion. Here we suggest that preionization is important to reach higher charge densities. To evaluate this hypothesis, we recorded the ion yields from toluene and *o*-nitrotoluene as a function of laser peak intensity using TL pulses (see Figure S8). For both molecules, it can be seen that molecular ionization starts at 10^{14} W/cm^2 and saturates soon after. Preionization is also expected to enhanced electron density localization near the nuclei.

Taking prealignment, bond softening, and preionization into account, we were surprised that we do not see larger differences between negative and positive TOD. We expected a greater difference. In the search for that difference, we carried out pump−probe experiments by generating a weak long pulse (∼100−200 fs) and a stronger (∼10 times more intense) short pulse (50 fs). However, the ion yield differences were slightly higher when the long pulse precedes the short one, which is similar to the negative TOD enhancement compared to positive TOD. We also evaluated fifth-order dispersion pulses that closely matched the pedestal of the FOD pulses and again failed to see large differences between positive and negative fifth order dispersion. Our findings show that FOD, which is time symmetric, produced the highest ion yields and KER values. From which it can be surmised that even a lagging pedestal is effective. Therefore, we propose our results require we consider a process known as cascaded ionization.[47,48] We envision that at the intensities being studied, a number of electrons move in response to the field, the cascaded hopping of electrons within these large molecules leads to the creation of highly charged ions such as C^{3+}, and their emission along the polarization direction of the laser pulses.

DOI: 10.1021/acs.jpca.6b08659
J. Phys. Chem. A 2016, 120, 8529−8536

CONCLUSIONS

We have explored the dissociative ionization of a number of molecules including acetylene, methanol, methylene chloride, acetonitrile, toluene and *o*-nitrotoluene following interaction with intense laser pulses in the presence and absence of high order dispersion. We find that both third- and fourth-order dispersion leads to an order of magnitude increases in the yield of fragment ions and that these enhancements are accompanied by a factor of 3 increase in the kinetic energy release of these ions; a factor of 2 increase for the smaller molecules. Comparison between pulses with pre- and postpedestals found relatively small differences, implying that mechanisms such as prealignment, preionization, and bond softening appear to play a relatively small role in explaining our results. We invoke a cascaded ionization process, in which multiple electrons hop within the molecule causing highly charged species. Once the electron cloud forms, it creates a localized plasma that is highly susceptible to the laser field and hence to the trailing pulse pedestal. This explanation is consistent with the detection of highly charged species such as C^{3+} emitted along the laser polarization axis, the minuscule difference between pre- and postpedestal pulses, and the molecular size dependence. We have found that the effects are greater for larger molecules. Future work will focus on molecular properties that enhance our findings. Similarly, we will explore the use of differently shaped pulses that may best take advantage of cascaded ionization. In particular, we are eager to explore stretched square pulses that offer fast initial ionization and maintain the field intensity constant until the end of the pulse.[49] Through collaborations, we hope to explore time-dependent theoretical simulation of our results and coincidence measurements that will further clarify the processes leading to high-energy highly charged particles.

ASSOCIATED CONTENT

Supporting Information

The Supporting Information is available free of charge on the ACS Publications website at DOI: 10.1021/acs.jpca.6b08659.

Laser spectrum and fidelity measurement, MICS AC for the TOD pulses pedestals, *o*-nitrotoluene mass spectrum, ion yields and KER for different beam polarizations, ion yield for toluene using different TL pulse durations, and ion yields as a function of peak intensity (PDF)

AUTHOR INFORMATION

Corresponding Author

*(M.D.) E-mail: dantus@msu.edu. Telephone: +1 (517) 353-1191.

Notes

The authors declare no competing financial interest.

ACKNOWLEDGMENTS

The authors are grateful for the financial support of this work on the behavior of molecules under intense fields from the Chemical Sciences, Geosciences and Biosciences Division, Office of Basic Energy Sciences, Office of Science, U.S. Department of Energy, DOE SISGR (DE-SC0002325). General discussion and comments from Dr. Nagitha Ekanayake are appreciated. We would also like to thank Nicholas Weingartz, Elena Bongiovanni, and Jeremy Lantis for their help.

REFERENCES

(1) Giusti-Suzor, A.; Mies, F. H.; DiMauro, L. F.; Charron, E.; Yang, B. Dynamics of H^{2+} in Intense Laser Fields. *J. Phys. B: At., Mol. Opt. Phys.* **1995**, *28*, 309−339.
(2) Yamanouchi, K. The Next Frontier. *Science* **2002**, *295*, 1659−1660.
(3) Posthumus, J. H. The Dynamics of Small Molecules in Intense Laser Fields. *Rep. Prog. Phys.* **2004**, *67*, 623−665.
(4) Esry, B. D.; Sayler, A. M.; Wang, P. Q.; Carnes, K. D.; Ben-Itzhak, I. Above Threshold Coulomb Explosion of Molecules in Intense Laser Pulses. *Phys. Rev. Lett.* **2006**, *97*, 013003.
(5) Lozovoy, V. V.; Zhu, X.; Gunaratne, T. C.; Harris, D. A.; Shane, J. C.; Dantus, M. Control of Molecular Fragmentation Using Shaped Femtosecond Pulses. *J. Phys. Chem. A* **2008**, *112*, 3789−3812.
(6) Konar, A.; Shu, Y.; Lozovoy, V. V.; Jackson, J. E.; Levine, B. G.; Dantus, M. Polyatomic Molecules under Intense Femtosecond Laser Irradiation. *J. Phys. Chem. A* **2014**, *118*, 11433−11450.
(7) Smith, B. H.; Compton, R. N. Laser Multiphoton Ionization of Tetrakis(dimethylamino)ethylene. *J. Phys. Chem. A* **2014**, *118*, 7288−7296.
(8) Gong, X.; Kunitski, M.; Betsch, K. J.; Song, Q.; Schmidt, L. P. H.; Jahnke, T.; Kling, N. G.; Herrwerth, O.; Bergues, B.; Senftleben, A.; et al. Multielectron Effects in Strong-field Dissociative Ionization of Molecules. *Phys. Rev. A: At., Mol., Opt. Phys.* **2014**, *89*, 043429.
(9) Hasegawa, H.; Hishikawa, A.; Yamanouchi, K. Coincidence Imaging of Coulomb Explosion of CS_2 in Intense Laser Fields. *Chem. Phys. Lett.* **2001**, *349*, 57−63.
(10) Comstock, M.; Senekerimyan, V.; Dantus, M. Ultrafast Laser Induced Molecular Alignment and Deformation: Experimental Evidence from Neutral Molecules and from Fragment Ions. *J. Phys. Chem. A* **2003**, *107*, 8271−8281.
(11) Roither, S.; Xie, X.; Kartashov, D.; Zhang, L.; Schöffler, M.; Xu, H.; Iwasaki, A.; Okino, T.; Yamanouchi, K.; Baltuska, A.; et al. High Energy Proton Ejection from Hydrocarbon Molecules Driven by Highly Efficient Field Ionization. *Phys. Rev. Lett.* **2011**, *106*, 163001.
(12) Xie, X.; Roither, S.; Schöffler, M.; Lötstedt, E.; Kartashov, D.; Zhang, L.; Paulus, G. G.; Iwasaki, A.; Baltuška, A.; Yamanouchi, K.; et al. Electronic Predetermination of Ethylene Fragmentation Dynamics. *Phys. Rev. X* **2014**, *4*, 021005.
(13) Wu, H.; Zhang, S.; Zhang, J.; Yang, Y.; Deng, L.; Jia, T.; Wang, Z.; Sun, Z. Observation of Hydrogen Migration in Cyclohexane under an Intense Femtosecond Laser Field. *J. Phys. Chem. A* **2015**, *119*, 2052−2057.
(14) Voronova, K.; Mozaffari Easter, C. M.; Covert, K. J.; Bodi, A.; Hemberger, P.; Sztáray, B. Dissociative Photoionization of Diethyl Ether. *J. Phys. Chem. A* **2015**, *119*, 10654−10663.
(15) Kübel, M.; Siemering, R.; Burger, C.; Kling, N. G.; Li, H.; Alnaser, A. S.; Bergues, B.; Zherebtsov, S.; Azzeer, A. M.; Ben-Itzhak, I.; et al. Steering Proton Migration in Hydrocarbons Using Intense Few-Cycle Laser Fields. *Phys. Rev. Lett.* **2016**, *116*, 193001.
(16) Assion, A.; Baumert, T.; Bergt, M.; Brixner, T.; Kiefer, B.; Seyfried, V.; Strehle, M.; Gerber, G. Control of Chemical Reactions by Feedback-Optimized Phase-Shaped Femtosecond Laser Pulses. *Science* **1998**, *282*, 919−922.
(17) Dantus, M.; Lozovoy, V. V. Experimental Coherent Laser Control of Physicochemical Processes. *Chem. Rev.* **2004**, *104*, 1813−1860.
(18) Alnaser, A. S.; Kübel, M.; Siemering, R.; Bergues, B.; Kling, N. G.; Betsch, K. J.; Deng, Y.; Schmidt, J.; Alahmed, Z. A.; Azzeer, A. M.; et al. Subfemtosecond Steering of Hydrocarbon Deprotonation through Superposition of Vibrational Modes. *Nat. Commun.* **2014**, *5*, 3800.
(19) Bohinski, T.; Moore Tibbetts, K.; Tarazkar, M.; Romanov, D. A.; Matsika, S.; Levis, R. J. Strong Field Adiabatic Ionization Prepares a Launch State for Coherent Control. *J. Phys. Chem. Lett.* **2014**, *5*, 4305−4309.
(20) Rudenko, A.; Zrost, K.; Feuerstein, B.; de Jesus, V. L. B.; Schröter, C. D.; Moshammer, R.; Ullrich, J. Correlated Multielectron

DOI: 10.1021/acs.jpca.6b08659
J. Phys. Chem. A 2016, 120, 8529−8536

Dynamics in Ultrafast Laser Pulse Interactions with Atoms. *Phys. Rev. Lett.* **2004**, *93*, 253001.
(21) Xie, X.; Roither, S.; Schöffler, M.; Xu, H.; Bubin, S.; Lötstedt, E.; Erattuphuza, S.; Iwasaki, A.; Kartashov, D.; Varga, K.; et al. Role of Proton Dynamics in Efficient Photoionization of Hydrocarbon Molecules. *Phys. Rev. A: At., Mol., Opt. Phys.* **2014**, *89*, 023429.
(22) Weiner, A. M. Femtosecond Pulse Shaping Using Spatial Light Modulators. *Rev. Sci. Instrum.* **2000**, *71*, 1929−1960.
(23) Pastirk, I.; Brown, E. J.; Zhang, Q.; Dantus, M. Quantum Control of the Yield of a Chemical Reaction. *J. Chem. Phys.* **1998**, *108*, 4375−4378.
(24) Itakura, R.; Yamanouchi, K.; Tanabe, T.; Okamoto, T.; Kannari, F. Dissociative Ionization of Ethanol in Chirped Intense Laser Fields. *J. Chem. Phys.* **2003**, *119*, 4179−4186.
(25) Yazawa, H.; Tanabe, T.; Okamoto, T.; Yamanaka, M.; Kannari, F.; Itakura, R.; Yamanouchi, K. Open-loop and Closed-loop Control of Dissociative Ionization of Ethanol in Intense Laser Fields. *J. Chem. Phys.* **2006**, *124*, 204314.
(26) Lev, U.; Graham, L.; Madsen, C. B.; Ben-Itzhak, I.; Bruner, B. D.; Esry, B. D.; Frostig, H.; Heber, O.; Natan, A.; Prabhudesai, V. S.; et al. Quantum Control of Photodissociation using Intense, Femtosecond Pulses Shaped with Third Order Dispersion. *J. Phys. B: At., Mol. Opt. Phys.* **2015**, *48*, 201001.
(27) Albeck, Y.; Kandhasamy, D. M.; Strasser, D. Multiple Detachment of the SF_6^- Molecular Anion with Shaped Intense Laser Pulses. *J. Phys. Chem. A* **2014**, *118*, 388−395.
(28) Xu, B.; Gunn, J. M.; Cruz, J. M. D.; Lozovoy, V. V.; Dantus, M. Quantitative Onvestigation of the Multiphoton Intrapulse Interference Phase Scan Method for Simultaneous Phase Measurement and Compensation of Femtosecond Laser Pulses. *J. Opt. Soc. Am. B* **2006**, *23*, 750−759.
(29) Coello, Y.; Lozovoy, V. V.; Gunaratne, T. C.; Xu, B.; Borukhovich, I.; Tseng, C.-h.; Weinacht, T.; Dantus, M. Interference Without an Interferometer: a Different Approach to Measuring, Compressing, and Shaping Ultrashort Laser Pulses. *J. Opt. Soc. Am. B* **2008**, *25*, A140−A150.
(30) Lozovoy, V. V.; Rasskazov, G.; Pestov, D.; Dantus, M. Quantifying Noise in Ultrafast Laser Sources and its Effect on Nonlinear Applications. *Opt. Express* **2015**, *23*, 12037−12044.
(31) Rasskazov, G.; Lozovoy, V. V.; Dantus, M. Spectral Amplitude and Phase Noise Characterization of Titanium-Sapphire Lasers. *Opt. Express* **2015**, *23*, 23597−23602.
(32) Walker, M. A.; Hansch, P.; Van Woerkom, L. D. Intensity-Resolved Multiphoton Ionization: Circumventing Spatial Averaging. *Phys. Rev. A: At., Mol., Opt. Phys.* **1998**, *57*, R701−R704.
(33) Hankin, S. M.; Villeneuve, D. M.; Corkum, P. B.; Rayner, D. M. Intense-Field Laser Ionization Rates in Atoms and Molecules. *Phys. Rev. A: At., Mol., Opt. Phys.* **2001**, *64*, 013405.
(34) Wang, P.; Sayler, A. M.; Carnes, K. D.; Esry, B. D.; Ben-Itzhak, I. Disentangling the Volume Effect Through Intensity-Difference Spectra: Application to Laser-Induced Dissociation of H^{2+}. *Opt. Lett.* **2005**, *30*, 664−666.
(35) Pestov, D.; Lozovoy, V. V.; Dantus, M. Multiple Independent Comb Shaping (MICS): Phase-only Generation of Optical Pulse Sequences. *Opt. Express* **2009**, *17*, 14351−14361.
(36) Kaziannis, S.; Kotsina, N.; Kosmidis, C. Interaction of Toluene with Two-color Asymmetric Laser Fields: Controlling the Directional Emission of Molecular Hydrogen Fragments. *J. Chem. Phys.* **2014**, *141*, 104319.
(37) Papadopoulou, C. C.; Kaziannis, S.; Kosmidis, C. Probing the Dynamics of Highly Excited Toluene on the fs Timescale. *Phys. Chem. Chem. Phys.* **2015**, *17*, 31727−31734.
(38) *NIST Chemical Webbook, NIST Standard Reference Database Number 69*; 1998.
(39) Lozovoy, V. V.; Dantus, M. Laser Control of Physicochemical Processes; Experiments and Applications. *Annu. Rep. Prog. Chem., Sect. C: Phys. Chem.* **2006**, *102*, 227−258.
(40) Thissen, R.; Delwiche, J.; Robbe, J. M.; Duflot, D.; Flament, J. P.; Eland, J. H. D. Dissociations of the Ethyne Dication $C_2H_2^{+2}$. *J. Chem. Phys.* **1993**, *99*, 6590−6599.
(41) Siozos, P.; Kaziannis, S.; Kosmidis, C. Multielectron Dissociative Ionization of CH_3I Under Strong Picosecond Laser Irradiation. *Int. J. Mass Spectrom.* **2003**, *225*, 249−259.
(42) Hansen, J. L.; Holmegaard, L.; Nielsen, J. H.; Stapelfeldt, H.; Dimitrovski, D.; Madsen, L. B. Orientation-Dependent Ionization Yields from Strong-Field Ionization of Fixed-in-Space Linear and Asymmetric Top Molecules. *J. Phys. B: At., Mol. Opt. Phys.* **2012**, *45*, 015101.
(43) Seideman, T.; Ivanov, M. Y.; Corkum, P. B. Role of Electron Localization in Intense-Field Molecular Ionization. *Phys. Rev. Lett.* **1995**, *75*, 2819−2822.
(44) Lötstedt, E.; Kato, T.; Yamanouchi, K. Efficient Ionization of One-Dimensional Acetylene Investigated by Time-Dependent Hartree-Fock Calculations. *Phys. Rev. A: At., Mol., Opt. Phys.* **2012**, *86*, 023401.
(45) Bubin, S.; Atkinson, M.; Varga, K.; Xie, X.; Roither, S.; Kartashov, D.; Baltuška, A.; Kitzler, M. Strong Laser-Pulse-Driven Ionization and Coulomb Explosion of Hydrocarbon Molecules. *Phys. Rev. A: At., Mol., Opt. Phys.* **2012**, *86*, 043407.
(46) Russakoff, A.; Bubin, S.; Xie, X.; Erattupuzha, S.; Kitzler, M.; Varga, K. Time-dependent Density-Functional Study of the Alignment-Dependent Ionization of Acetylene and Ethylene by Strong Laser Pulses. *Phys. Rev. A: At., Mol., Opt. Phys.* **2015**, *91*, 023422.
(47) Pegarkov, A. I. Electron Excitation and Cascade' Ionization of Diatomic Molecules with Ultra-Short Pulses of Strong IR Lasers. *Chem. Phys. Lett.* **2001**, *343*, 642−648.
(48) Sakabe, S.; Nishihara, K.; Nakashima, N.; Kou, J.; Shimizu, S.; Zhakhovskii, V.; Amitani, H.; Sato, F. The Interactions of Ultra-Short High-Intensity Laser Pulses with Large Molecules and Clusters: Experimental and Computational Studies. *Phys. Plasmas* **2001**, *8*, 2517−2524.
(49) Lozovoy, V. V.; Rasskazov, G.; Ryabtsev, A.; Dantus, M. Phase-Only Synthesis of Ultrafast Stretched Square Pulses. *Opt. Express* **2015**, *23*, 27105−27112.

DOI: 10.1021/acs.jpca.6b08659
J. Phys. Chem. A 2016, 120, 8529−8536